High speed tangential soft x-ray camera for the study of magnetohydrodynamics instabilities

S. von Goeler, R. Kaita, M. Bitter, G. Fuchs, M. Poier, G. Bertschinger, H. R. Koslowski, K. Toi, S. Ohdachi, and A. Donné

Citation: Review of Scientific Instruments **70**, 599 (1999);
View online: https://doi.org/10.1063/1.1149382
View Table of Contents: http://aip.scitation.org/toc/rsi/70/1
Published by the American Institute of Physics

High speed tangential soft x-ray camera for the study of magnetohydrodynamics instabilities

S. von Goeler, R. Kaita, and M. Bitter
Princeton Plasma Physics Laboratory, Box 451, Princeton, New Jersey 08543

G. Fuchs, M. Poier, G. Bertschinger, and H. R. Koslowski
Institut für Plasmaphysik, Association Euratom KFA, partner in the Trilateral Euregio Cluster, Forschungszentrum Jülich GmbH, D52425 Jülich, Germany

K. Toi and S. Ohdachi
National Institute for Fusion Studies, Toki-shi 509-52, Japan

A. Donné
FOM-Instituut voor Plasmafysica Rijnhuizen, Association Euratom FOM, partner in the Trilateral Euregio Cluster, Box 1207, 3430 BE Nieuwegein, Holland

(Presented on 9 June 1998)

A fast camera system is being prepared for the TEXTOR tokamak for the investigation of magnetohydrodynamics (MHD) instabilities. The camera will consist of a scintillator screen for conversion of x rays into visible light, a fiberoptic cable for transport of the visible images out of the Textor magnetic field, an electrostatic image converter for amplification and demagnification of the images, and a fast charge-coupled device (CCD) camera for capturing and storing the image data. The purpose of our camera is two-dimensional imaging of magnetic islands and the structure of MHD instabilities. In order to increase the signal intensity and simultaneously reduce statistical noise, we maximize the diameter of the scintillator screen to 100 mm. For good time response, we use fast scintillators and phosphors, and plan to employ a 1 MHz framing CCD camera. MHD events having an amplitude larger than 1% can be observed with a time resolution of 100 kHz and a spatial resolution of 3 cm. In the future, the camera will be used on the Large Helical Device in Japan. © *1999 American Institute of Physics.* [S0034-6748(99)62201-8]

I. INTRODUCTION: ADVANTAGES OF FAST TANGENTIAL IMAGING

X-ray imaging diagnostics for the investigation of magnetohydrodynamics (MHD) instabilities are widely used on all major tokamaks. They usually consist of a row of silicon diodes that look at the plasma in a poloidal cross section perpendicular to the magnetic field.[1] These one-dimensional (1D) arrays actually provide two-dimensional (2D) information, because tokamak plasmas tend to rotate. As in the well-known medical CAT scans, the rotation of a MHD instability in front of a 1D detector array permits to perform 2D reconstructions, and one determines in this way, for example, the toroidal and poloidal wavelengths of tearing modes and reconstructs their magnetic islands.[2,3] However, since conventional x-ray imaging is not truly two-dimensional, there are major shortcomings to this approach:

(1) For fast phenomena, e.g., for instabilities occurring on a time scale shorter than the rotation period, one does not obtain two-dimensional information. For example the sawtooth crash[4] is today, after 24 years of intensive research, still not fully understood.[5]

(2) Traditional x-ray imaging also does not provide 2D information for phenomena, which do not participate in the plasma rotation. Such phenomena include magnetic islands created by external coils or error fields, certain stationary MHD instabilities known as locked modes,[6] and multifaceted asymmetric radiation from the edge (MARFEs).[7]

(3) Conventional x-ray imaging has one more serious shortcoming it is insensitive to plasma perturbations with short poloidal wave length. X-ray signals are proportional to the integral over the x-ray emissivity along a line of sight, and the insensitivity to short poloidal wavelengths is a direct consequence of this fact. We try to illustrate this in Fig. 1: For the low-*m* MHD mode in subfigure (a), a perpendicular view with respect to the magnetic field gives satisfactory results, i.e., the ratio $\Delta I/I$, where I is the line integrated signal and ΔI the perturbation caused by the MHD instability, has roughly

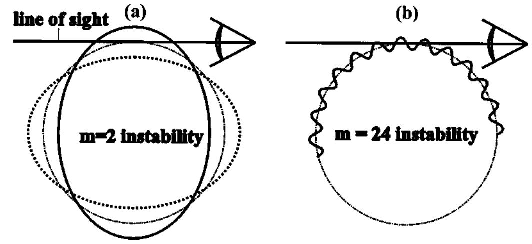

FIG. 1. The effects of line integration in 1D imaging. The $m=2$ MHD mode (a) shows up prominently on the chord-integrated signals. The amplitude of a $m=25$ mode (b) is strongly suppressed, because the contributions from the many maxima and minima cancel out.

the same size as the ratio $\Delta\epsilon/\epsilon$ for the local x-ray emissivity ϵ. On the other hand, for the high m mode in subfigure (b), the contributions by the many maxima and minima tend to cancel during line integration, and $\Delta I/I \ll \Delta\epsilon/\epsilon$. This cancellation can be avoided with a tangential view (i.e., a view, where the lines of sight cut through the paper plane), because sight lines tend in this case to follow the (predominantly toroidal) magnetic field lines, and because plasma parameters remain constant on a field line during MHD instabilities. A simulation of 2D tangential imaging[8] has shown that MHD modes with very high poloidal wave number m, for example $m=20$ or 30, can still be resolved with good accuracy.

It has been attempted to overcome these difficulties by installing several linear arrays in a poloidal plane. However, installation of even ten linear arrays[9]—although unquestionably a large improvement—does not seem to permit analysis of the very small poloidal wave lengths. In our work on the TEXTOR tokamak facility in Jülich, we try to undertake the next logical step and construct a truly two-dimensional, fast, tangential soft x-ray camera (TSXC).

In Sec. II we present a mechanical layout of the TSXC. In Sec. III we estimate the statistical x-ray photon noise. In Sec. IV we discuss the transport of the visible image out of the magnetic field, and, finally, give a status report of the TSXC project in Sec. V.

II. MECHANICAL LAYOUT OF THE TANGENTIAL SOFT X-RAY CAMERA ON TEXTOR

The design of the TEXTOR TSXC has been inspired by the first two-dimensional soft x-ray camera, which was built by Fonck[10] for measuring the bean-shaped magnetic flux surfaces of the Princeton Beta Experiment (PBX). A modified version of this camera was later used on PBX-*M* to diagnose hard x-ray emission from suprathermal electrons during lower hybrid current drive.[11] The camera is a pinhole camera. The x-ray image is converted into a visible image by a scintillator screen. The visible image is transported out of the magnetic field by a fiberoptic bundle, demagnified, amplified, and recorded by a fast charge-coupled device (CCD) camera. The challenge has been to increase the framing speed from 300 Hz (PBX) to 300 kHz (TEXTOR), in order to make the concept suitable for MHD instability studies.

Subfigure (a) of Fig. 2 shows the mechanical layout of the camera on TEXTOR. The pinhole of the camera is located at a major radius R of 2.854 m at a height of 0.216 m above the horizontal midplane of the tokamak. Basically the camera can see most of the plasma cross section, however, there is presently interference with the TEXTOR inner liner for minor radii larger than 0.30 m. This will be corrected at a later time by enlarging the viewing hole in the inner liner at that port location. The circular pinhole is interchangeable from 1 to 5 mm diameter. A thin beryllium absorber foil, close to the pinhole, shields out visible and UV light. The foil consists of a 0.5 μm thin Be foil with a 0.1 μm layer of LiF. The latter closes a beryllium transmission window below the 112 eV Be K-edge. The fiberoptic faceplate[12] which carries the scintillator, serves also as a vacuum interface. It is sealed by a viton O ring

.

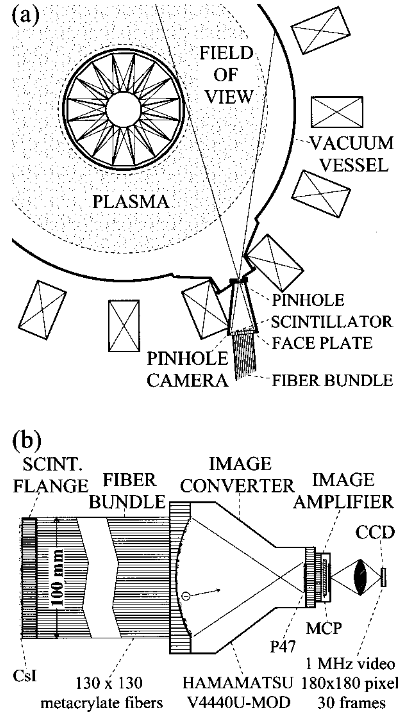

FIG. 2. Schematic layout of the tangential soft x-ray camera on TEXTOR.

Subfigure (b) shows the optical setup of the TSXC. X-ray photons impinge on the scintillator layer on the left. Medical image converters generally use CsI($T1$) as scintillator. However, since CsI is hygroscopic and requires sensitive handling, we will use initially the much cheaper and simpler-to-handle P47 phosphor. Both have very fast decay times <2 μs. The scintillator is deposited on a 120 mm diam glass faceplate.[13] The fibers have a diameter of 15 μm and the numerical aperture is 1.0. The face plate is connected to a coherent fiberoptic bundle,[13] which transports the image out of the TEXTOR magnetic field. The 100 mm bundle is 2.0 m long and consists of 75 mm metacrylate fibers. The fiberoptic bundle is connected on the other end to a first-generation image converter, which amplifies the image and provides a 4:1 demagnification. The Hamamatsu model #4440U-MOD tube possesses the largest (100 mm diam), commercially available input window. It has a P47 phosphor screen of 25 mm diameter deposited on a fiberoptic output window.

Two data acquisition systems are under discussion for the TSXC. Both consist of a fast image intensifier and a CCD camera. The CCD camera, which we ultimately propose for this application, has on-chip data storage.[14] The principle is shown in Fig. 3. The chip consists of 180×180 superpixels, of which four are shown. The light is detected by a photodiode, which—for detection efficiency—covers a large part (34%) of the surface area of a superpixel. Charges produced in the photodiode are routed via gate 2 and 3 to the memory area or via gate 1 to a dump. The movement of charge from one memory pixel to the next can be accom-

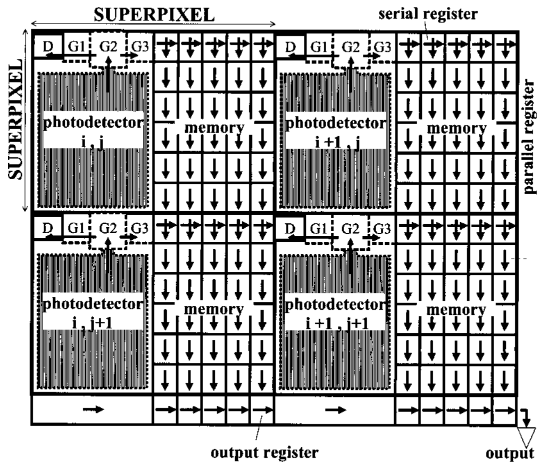

FIG. 3. Principle of the PSI fast-framing CCD camera with on-chip memory storage.

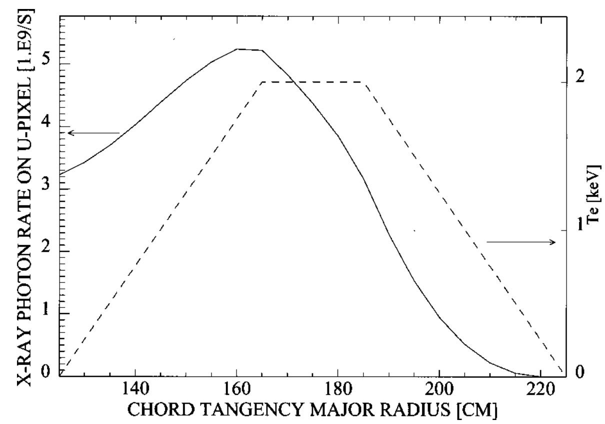

FIG. 4. Computed x-ray intensity on a pixel of area $5\times5\ \mathrm{mm}^2$ on the scintillator screen vs major radius R for the TSXC on TEXTOR. For the simulation, trapezoidal density and electron temperature profiles (dashed curve) were used.

plished in the time period of 1 μs. In this way 32 frames can be acquired at a rate of 1 MHz. When the memory is full, the chip is read out at a slow rate. The camera can be pre- and posttriggered. The PSI camera is expensive and has not been purchased yet. In order to test the TSXC concept, we use a normal ICCD (Hamamatsu model No. C4077-02). It has a high speed MCP shutter (100 ns–14 ms) and obtains one frame every 16 ms. The data are recorded by a LeRoy model No. 6810 ADC driven by a TV clock generator (CPS 312).

III. X-RAY PHOTON STATISTICS

The x-ray signal intensity in a 2D tangential pinhole camera with a circular pinhole is smaller than the intensity in a conventional 1D diode array, where in general a slot aperture is employed. Therefore, one must estimate the x-ray intensity accurately and make sure that statistical x-ray noise is sufficiently small. For a realistic calculation, we consider plasma continuum radiation, i.e., bremsstrahlung and recombination radiation, described by the formula[15]

$$\frac{dP_{\mathrm{ff+fb}}}{dh\nu}\left[\frac{1}{\mathrm{cm}^3\ \mathrm{s}}\right]=3.0\times10^{11}\ \frac{1}{\sqrt{T_e/\mathrm{keV}}}\times\gamma(T_e,Z)Z_{\mathrm{eff}}\ \frac{n_e^2}{10^{26}\ \mathrm{cm}^6}\exp\left(-\frac{h\nu}{kT_e}\right),$$

where P is the radiated power, $h\nu$ the photoenergy, T_e the electron temperature, Z_{eff} the average plasma ion charge, and n_e the electron density. The factor γ describes the enhancement of the radiation over bremsstrahlung due to free-bound (recombination) radiation. It is assumed to be caused predominantly by highly ionized carbon. The exact amount of recombination radiation depends on the charge state distribution of the carbon, which varies with plasma conditions and depends on carbon particle transport. Since we need only a crude estimate, we use an approximate formula

$$\gamma(T_e)=1.0+29.0\ \exp\{-(2.75-1.1[T_e/\mathrm{keV}]^{-0.4})^2\}.$$

With the help of these equations, the photon emissivity ϵ_{ph} is calculated as a function of minor radius r,

$$\frac{\epsilon_{\mathrm{ph}}}{\mathrm{cm}^{-3}\ \mathrm{s}^{-1}}=\int_{E_{\mathrm{cut}}}^{\infty}\frac{1}{h\nu}\frac{dP}{dh\nu}\,dh\nu=3\times10^{11}\ \frac{1}{\sqrt{T_e/\mathrm{keV}}}\ \gamma Z_{\mathrm{eff}}\ \frac{n_e^2}{10^{26}\ \mathrm{cm}^{-6}}\ E_1\left(\frac{E_{\mathrm{cut}}}{kT_e}\right).$$

Here, E_{cut} is the low energy cutoff of the Be foil and E_1 the exponential integral of order 1. The x-ray photon brightness, b_{ph}, in the midplane of the tokamak, becomes

$$b_{\mathrm{ph}}(R_{\mathrm{tg}})=\int\epsilon_{\mathrm{ph}}ds=\int_{R_{\mathrm{tg}}}^{R_0+a}\epsilon_{\mathrm{ph}}(R-R_0)(1/\sqrt{R^2-R_{\mathrm{tg}}^2})2RdR,$$

where R is the major radius of the tokamak, and R_{tg} is the tangency major radius of the sight line. Since we are concerned only with intensity estimates, we use simple trapezoidal profiles for both the plasma electron temperature and density (see Fig. 4). The number of x-ray photons dN_{ph} that impinge on a pixel of area $A_d=a_d^2$ from a small plasma volume element dV in clear view of the pixel, i.e., on its sight line, is given by

$$d\dot{N}_{\mathrm{ph}}=\epsilon(r)dV\ \Delta\Omega/(4\pi)=\epsilon(r)dV\ A_d/(4\pi D^2)=\epsilon(r)(\pi/4)a_c^2\ ds\ A_d/(4\pi D^2).$$

Here, $\Delta\Omega$ is the spatial angle, under which the pixel appears from dV, D is the distance between the pixel and the emitting volume dV, and ds a length element along the sight line. From geometrical considerations, the projected diameter a_c of the pinhole (diameter a_p) can be expressed in the form $a_c=a_p(D-d)/d\sim a_pD/d$, where d is the distance between the pixel and the pinhole (i.e., approximately the distance pinhole scintillator screen). The total number of photons N_{ph} that hit the pixel is hence

$$\dot{N}_{ph} = b_{ph} a_p^2 a_d^2 / (16 d^2).$$

For convenience we choose $a_p = a_d$. Now we maximize the intensity, keeping the full width at half maximum spatial resolution in the plasma L_r fixed,

$$L_r = a_p (D/d) = \text{const.}$$

For small cameras the quantity D remains nearly constant, and hence also the ratio a_p/d. By increasing d, we can open up the pinhole aperture a_p proportionally, and the intensity increases as the area of the pinhole. In other words, the larger the camera dimensions the larger the x-ray intensity. We look consequently for devices with the largest possible scintillator screen. The Hamamatsu tube has the largest, commercially available input window. In Fig. 4, we show the calculated x-ray intensity for the TEXTOR TSXC in the horizontal midplane. For the computations we assumed a pinhole aperture a_p of 5 mm diameter; this corresponds to a resolution of 3.5 cm in the plasma. The x-ray cutoff E_{cut} was 1 keV, the central plasma density $n_{e0} = 4.0 \times 10^{13}$ cm^{-3}, $T_{e0} = 2$ keV, and $Z_{eff} = 2$. As shown in Fig. 4, the number of x-ray photons from the plasma core, which hit a 5×5 mm^2 ''pixel,'' is approximately 4×10^9 s^{-1}. As a consequence, the x-ray statistical noise will be 0.5% if one measures with a sampling rate of 100 kHz.

IV. IMAGE TRANSPORT OUT OF THE MAGNETIC FIELD

The x-ray intensity for the TSXC camera is only marginally sufficient. We have to make sure that extra noise is not generated further down in the data acquisition chain. A critical condition is that every x-ray photon produces at least one photoelectron in the Hamamatsu image converter tube. A crude estimate shows that this condition is not quite fulfilled for our camera: The efficiency of x-ray to light conversion in P47, the scintillator that we intend to use for first operation, is approximately 6.3%, i.e., a 1.5 keV x-ray photon produces approximately 33 scintillation photons at a wavelength of 4100 Å. Only half of these photons are directed towards the face plate and only 75% are accepted by it because of the packing fraction and the cladding. There is only negligible light loss in the fiberoptic cable, but there occurs a loss at every interface, i.e., at the transition from the faceplate to the fiberoptic cable and at the transition from the fiberoptic cable to the image intensifier. At the first interface the intensity is reduced by 15% because of the packing fraction, and by a factor of 5 because the numerical aperture of the plastic fibers is only 0.5, compared to 1.0 of the face plate. Another 25% is lost at the second interface. The quantum efficiency of the photo cathode of the tube at 4100 Å is 10%. Summing up, every 1.5 keV x-ray photon produces only 0.16 photoelectrons in the image converter tube, and it is likely, that the transport of the image out of the magnetic field increases the photon noise by a factor of 2.5. The estimate is obviously crude. However, it is not easy to improve it. The luminous efficiency of phosphors interacting with 1–3 keV x-ray photons is not very well known. We use values extrapolated from 10 keV electron impact data. The scintillator screen has a thin Al reflection layer that increases the light output. We did not take this effect into account, because there are other processes that decrease the output, for instance scattering, reflection, or absorption of the scintillation light by the scintillator grains. These complex phenomena are hard to model exactly.

V. STATUS OF THE TSXC PROJECT ON TEXTOR

At the moment the fast tangential soft x-ray camera is being assembled at the Institute for Plasma Physics at Jülich. The mechanical design is complete, and the camera components are manufactured in the workshops at the Forschungszentrum. The scintillator flange and the fiberoptic bundle have been ordered. The image converter tube and ICCD have been purchased and have been tested in Japan and in Jülich. The camera is scheduled for laboratory tests, and will then be moved and connected to TEXTOR. Operation on TEXTOR will begin after the summer machine opening in September 1998.

ACKNOWLEDGMENTS

The authors are grateful for the support of Dr. K. Young from PPPL, of Dr. U. Samm and Professor G. Wolf from the IPP Jülich, and of Professor F. C. Schüller from the FOM Instituut. E. Kemmereit performs the mechanical design and R. Lemmens provides technical assistance. This project is supported by the U.S. Department of Energy Contract No. DE-AC02-76-CHO-3073, and by Euratom and the ''Nederlandse organisatie voor WetenschappelijkOnderzoek NWO.''

[1] K. Hill *et al.* Rev. Sci. Instrum. **56**, 830 (1985).
[2] S. von Goeler, Plasma Phys. Controlled Nucl. Fusion Res. **2**, 71 (1975).
[3] N. Sauthoff, S. von Goeler, and W. Stodiek, Nucl. Fusion **18**, 1445 (1978).
[4] S. von Goeler, W. Stodiek, and N. Sauthoff, Phys. Rev. Lett. **33**, 1201 (1974).
[5] H. Soltwisch, Plasma Phys. Controlled Nucl. Fusion Res. **34**, 1669 (1992).
[6] Takahashi, Fusion Eng. Des. **34/35**, 89 (1997).
[7] B. Lipschultz *et al.*, Nucl. Fusion **24**, 977 (1984).
[8] S. von Goeler *et al.*, Rev. Sci. Instrum. **61**, 3055 (1990).
[9] R. Granetz and J. Camacho, Nucl. Fusion **25**, 727 (1985).
[10] Ray Fonck *et al.*, Rev. Sci. Instrum. **59**, 1831 (1988).
[11] S. von Goeler *et al.*, Rev. Sci. Instrum. **65**, 1621 (1994).
[12] Manufactured by Incom Inc., 294 Southbridge Road, Charlton, MA 01507-5238.
[13] Manufactured by Inwave Corporation, 750 Commercial Street, Eugene, OR 94402.
[14] Princeton Scientific Instruments, Inc., 7 Deer Park Drive, Monmouth Junction, NJ 08852.
[15] S. von Goeler *et al.*, Nucl. Fusion **15**, 301 (1975).